

Phase and Amplitude Measurements of Coherent Optical Wavefronts

By JOSEPH T. RUSCIO

(Manuscript received March 24, 1966)

A phase-locked laser loop has been used as an amplitude and phase measuring device for coherent optical wavefronts. A relative phase resolution on the order of one degree and an amplitude resolution accurate to one dB or better were obtained. The system and measuring techniques used are described, and the results obtained are illustrated by several examples.

I. INTRODUCTION

A laser phase-locked loop¹ consisting of two laser oscillators has been used to measure the relative phase and amplitude of the wavefront of a laser beam. A phase resolution on the order of one degree and an amplitude accuracy better than one dB have been obtained. This system was used to analyze the optical qualities of devices placed in the beam's path by measuring their effect on the wavefront. The system and techniques used along with the results obtained are described and illustrated in this paper.

II. DESCRIPTION OF THE MODIFIED PHASE-LOCKED LASER LOOP

The phase-locked system is shown in Fig. 1. It consists of controlled and uncontrolled optical oscillators which are single-frequency helium-neon lasers operated at 6328Å. Details of the oscillators' characteristics are shown in Figs. 2 and 3. The beam waists and spot sizes are defined and calculated in Appendix A. The two lasers used initially are shown in Fig. 2; however, tube replacements required a different combination of mirrors to maintain a single transverse mode, so the final measurements were made with the lasers shown in Fig. 3. Results are identified with the lasers used.

Prior to combining the two beams (Fig. 1) on the surface of the photomultiplier by means of a mirror and a beam splitter, the output beam of

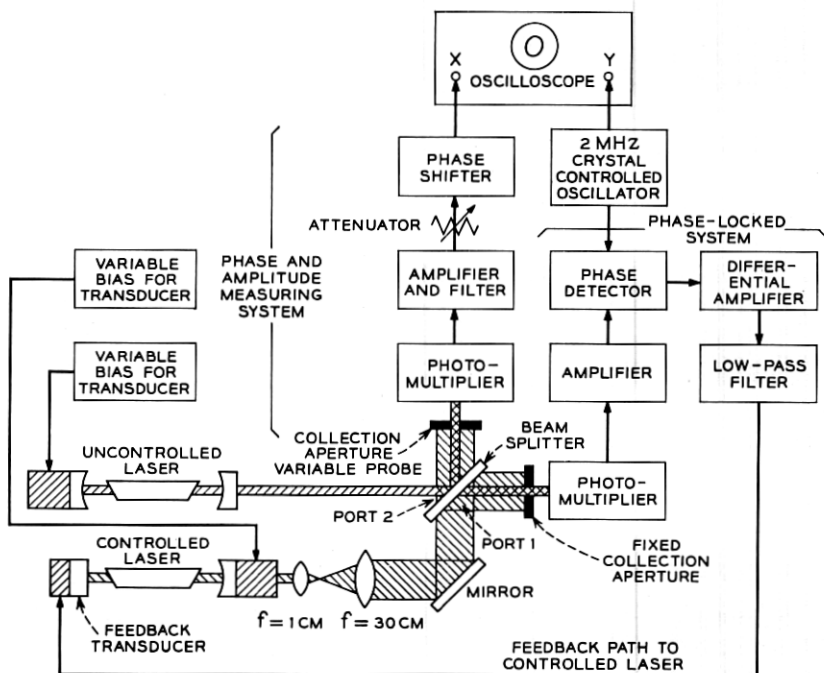


Fig. 1 — Phase-locked optical maser system.

the controlled laser, which will be referred to as the reference beam, is collimated by a telescope.

III. THEORY OF OPERATION

The beam splitter in Fig. 1 provides two outputs: Port 1 to phase-lock the system and Port 2 for making the phase and amplitude measurements. The photomultipliers are square law detectors. Thus, if the field at the photosensitive surface is

$$E = E_c \cos \omega_c t + E_u \cos \omega_u t$$

where

E_c is the controlled oscillator field amplitude,

E_u the uncontrolled oscillator field amplitude,

and

ω_c , ω_u the respective angular frequencies, then since E_c and E_u have the same polarization, the resulting photocurrent is proportional to

$$E^2 = \frac{1}{2}E_c^2 + E_c E_u \cos (\omega_c - \omega_u)t + \frac{1}{2}E_u^2 \quad (1)$$

which consists of a dc term $\frac{1}{2}(E_c^2 + E_u^2)$ plus the difference frequency term $[E_c E_u \cos(\omega_c - \omega_u)t]$.

In the original phase-lock loop,¹ the two lasers were locked at the same frequency with a dc error voltage proportional to their phase difference. When the loop locks, the controlled laser tracks the frequency of the uncontrolled laser in a manner such that the instantaneous phase error α remains smaller than 90° in absolute magnitude. A discussion of the phase relationships in the loop is given in Appendix B.

To improve the measurement of phase and amplitude, the laser oscillators were phase-locked at a fixed frequency difference of 2 MHz by using an additional phase detector with a 2-MHz crystal-controlled oscillator as a reference. When the lasers are tuned so that their difference frequency is 2 MHz, the 2-MHz output from the photomultiplier is amplified and applied to the phase detector. The phase detector output is a dc error voltage proportional to the phase difference between the 2-MHz beatnote and 2-MHz reference signal (Appendix B). This error voltage

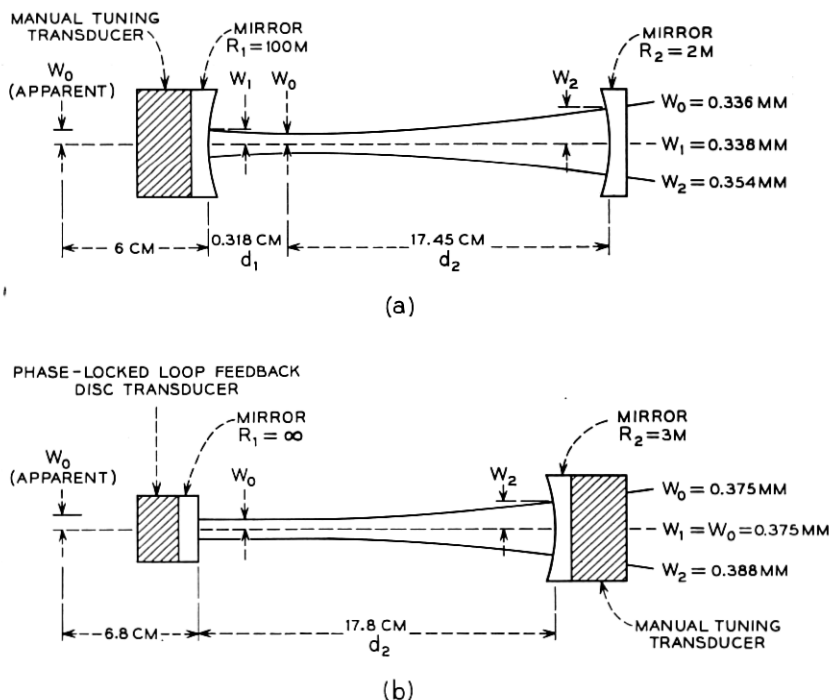


Fig. 2—Initial lasers; (a) uncontrolled laser oscillator (signal), (b) controlled laser oscillator (reference).

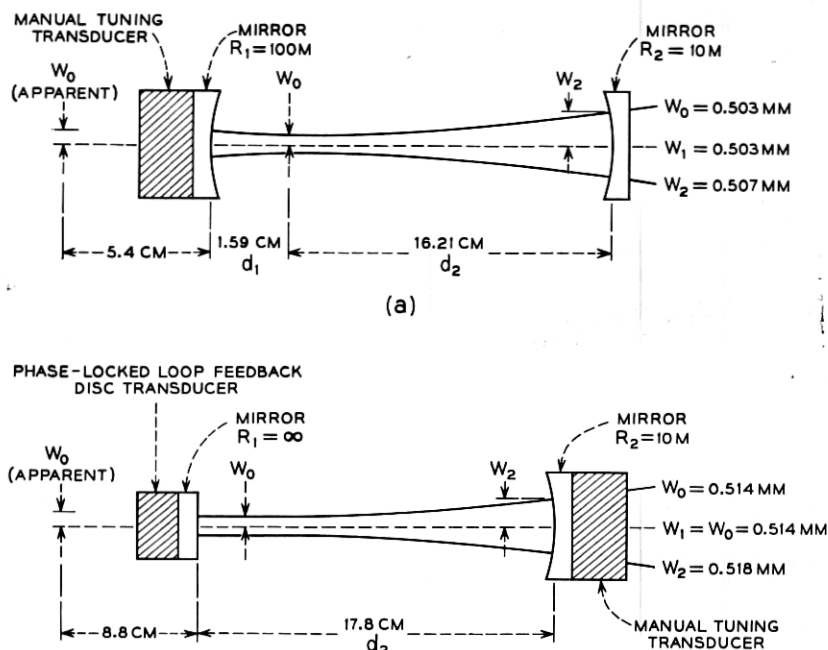


Fig. 3—Replacement lasers; (a) uncontrolled laser oscillator (signal), (b) controlled laser oscillator (reference).

is fed back through a differential amplifier to a piezoelectric disc transducer. A mirror mounted on this transducer forms one end of the controlled laser cavity. There is an additional transducer-mounted mirror on the other end of the laser cavity; this is used for initial tuning (see Figs. 2(b) and 3(b)). The error voltage causes the cavity length and hence the frequency to change in a direction such that the phase error is decreased. When the loop locks, the controlled laser tracks the frequency of the uncontrolled laser in a manner such that the instantaneous phase error between the two 2-MHz signals remains less than 90° . The loop tracks over a frequency range of $\pm 50\text{ MHz}$, based on a feedback voltage of $\pm 80\text{ volts}$ and a piezoelectric transducer having a sensitivity of 0.6 MHz/volt . This means that the phase difference between the reference signal and the beatnote signal remains less than 90° in absolute magnitude as long as the frequency of the uncontrolled laser does not vary more than $\pm 50\text{ MHz}$.

IV. TECHNIQUE OF MEASUREMENT

Port 2 of the beam splitter provides an output which is utilized for phase and amplitude measurements; this permits scanning the com-

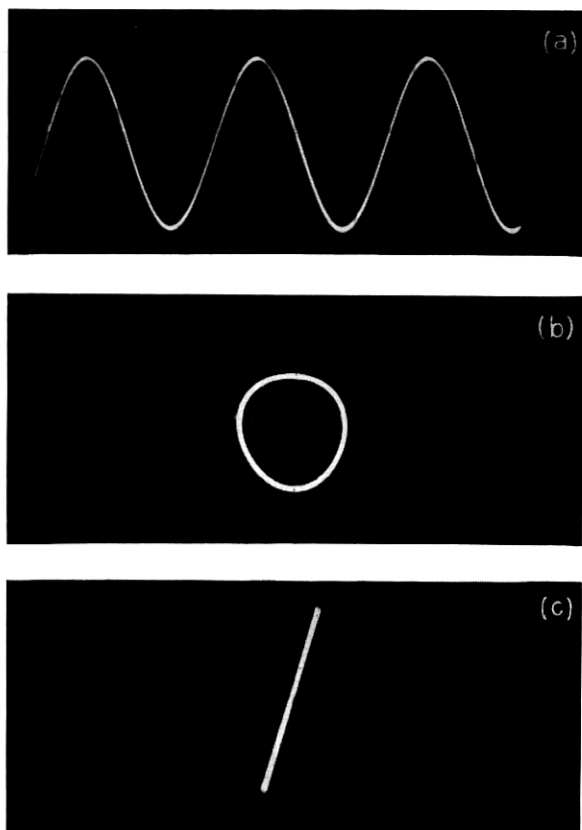


Fig. 4.— Beatnote (2 MHz) Lissajou; (a) 2-MHz Beatnote, (b) lissajou pattern indicating phase difference between two 2-MHz signals, (c) zero phase shift between two 2-MHz signals.

bined beams without interfering with the phase-locked loop. A circular collection aperture of a few mils diameter is used to scan the superimposed wavefronts, selecting the "point" area detected by the photomultiplier. The phase of the 2-MHz beatnote obtained from the photomultiplier is dependent on the position of the "point" area on the wavefronts. Frequency selective circuits, including a 2-MHz tuned circuit in the photomultiplier output and a crystal filter (2-MHz center frequency, 4-kHz bandwidth), assist in maintaining a signal-to-noise ratio that is better than 40 dB. The result is a well-defined 2-MHz signal (Fig. 4(a)), which with the 2-MHz reference can be used to produce Lissajou patterns, as in Figs. 4(b) and 4(c), on an oscilloscope. By this means relative phase measurements between the two beams are possible.

Distortion of the pattern in Fig. 4(b) is due to limitations in the horizontal amplifier of the oscilloscope. Measurement of the beatnote amplitude as a function of the probe position from the beam axis is used to determine the relative amplitude of the wavefronts. The techniques and theory used for both phase and amplitude measurements will be described.

V. PHASE MEASUREMENT

The phase measurement is based on the fact that each of the two spherical wavefronts of radii R_1 and R_2 can be expressed approximately as

$$E_1 = \exp(jkd^2/2R_1) = \exp(j\Phi_1),$$

where

$$\Phi_1 = (kd^2/2R_1),$$

d is the distance from the beam axis, and

$$k = 2\pi/\lambda.$$

$$E_2 = \exp(jkd^2/2R_2) + \gamma = \exp(j\Phi_2) + \gamma,$$

where

$$\Phi_2 = (kd^2/2R_2)$$

and γ is the phase difference between the two wavefronts on the axis. Thus, the phase difference between the two wavefronts is given by

$$\Delta\Phi = \Phi_2 - \Phi_1 + \gamma = (kd^2/2) (1/R_2 - 1/R_1) + \gamma.$$

The telescope reduces the divergence of the reference beam so that its radius of curvature,* R_1 , can be considered infinitely large, therefore,

$$\Phi_1 \approx 0$$

and

$$\Delta\Phi \approx (kd^2/2R_2) + \gamma.$$

From Fig. 5, it can be seen that if the phase shift as indicated by the Lissajou pattern is adjusted to be zero at the center of the beam (by means of an auxiliary phase shifter), all measurements can be made relative to this reference and the relative phase shift becomes

$$\Delta\Phi \approx (kd^2/2R_2).$$

* Calculations for the radii of curvature involved using the telescope are given in Appendix C.

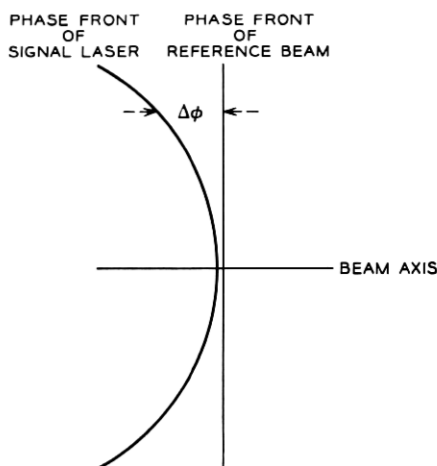


Fig. 5—Phase relationship between spherical and planar wavefronts.

Measurement of $\Delta\Phi$ as a function of distance (d) from the beam axis provides a means of determining R_2 .

The experimental layout for measuring the relative phase between the two beams is shown in Fig. 1. The movable collection aperture positioned directly in front of the photomultiplier can be moved in 5-mil increments along the horizontal or vertical axis. Changes in phase with position is plotted as shown in Figs. 6(a), (b) and 7(a), (b).

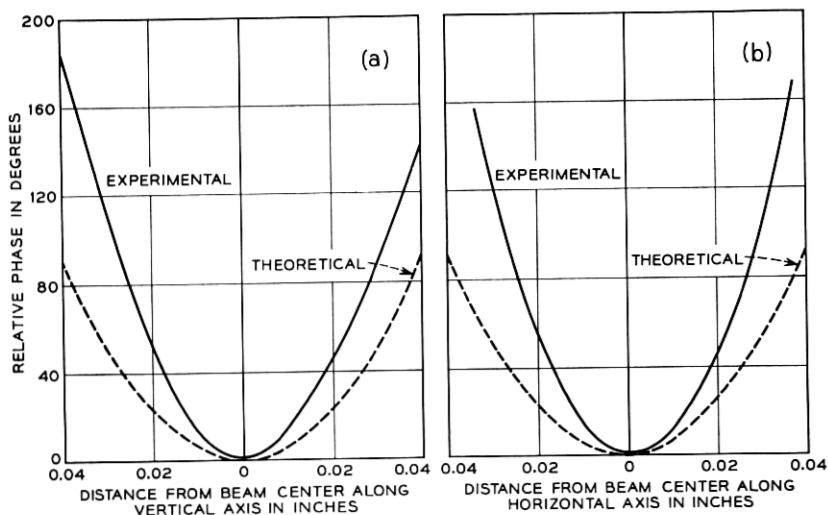


Fig. 6—Optical wavefronts (laser in Fig. 2(a)).

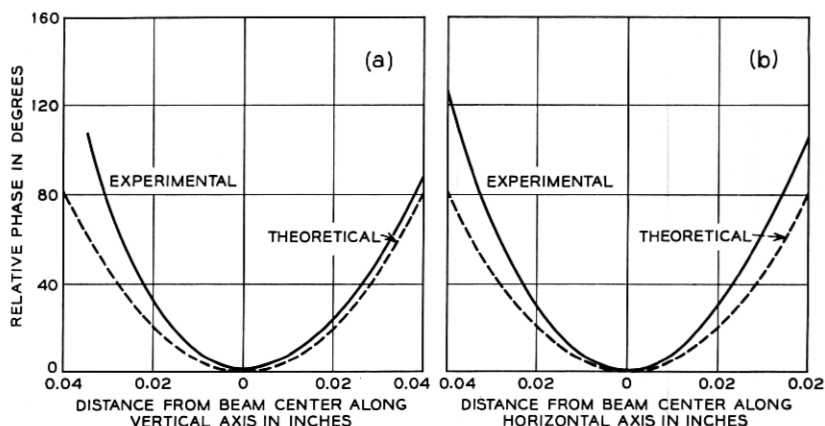


Fig. 7—Optical wavefronts (laser in Fig. 3(a)).

The curves in Figs. 6(a) and (b) are for the laser shown in Fig. 2(a). Measurement of the optical wavefront was made at a distance of 3 meters from the apparent beam waist using a 0.015-inch diameter collection aperture. Similar data for the laser in Fig. 3(a) are shown in Figs. 7(a) and (b) in which case the collection aperture diameter was 0.009 inch. Theoretical curves indicate radii of curvature less than the measured values for all cases. The radius of curvature at a distance z from the apparent beam waist location is given by²

$$R = z \left[1 + \left(\frac{z_0}{z} \right)^2 \right],$$

where $z_0 = \pi w_0^2 / \lambda$, w_0 being the beam-waist radius, and $\lambda = 0.6328\mu$.

The disagreement between the theoretical and experimental values has not been resolved. This problem remains under consideration as work continues in this area.

VI. FIELD AMPLITUDE MEASUREMENTS

In a similar manner, observing the 2-MHz beatnote amplitude as a function of probe distance perpendicular to the beam axis provides a means of determining the field amplitude distribution of the combined beams. With the reference beam enlarged, in this case to 30 times its initial size, the amplitude of the reference beam over the distance scanned is relatively constant; therefore, the amplitude distribution measured is, in fact, the relative amplitude of the signal beam. The accuracy is governed by the variation in intensity of the reference beam

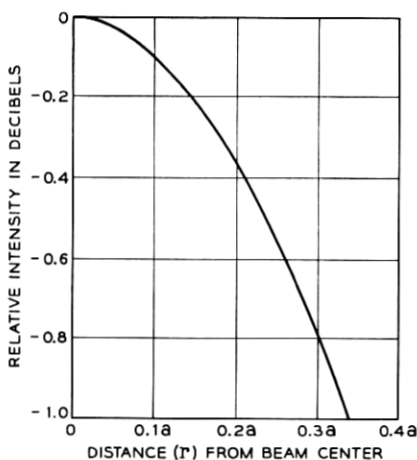
over the area scanned as shown in Fig. 8. With a beam reference spot size of 1-inch diameter, scanning a distance of $0.2a$ (a = beam radius) from the beam axis introduces an error of 0.4 dB in the relative measurements.

Examples of the measured amplitude distribution as a function of distance from the center of the beam are shown in Figs. 9(a), (b) and 10(a), (b). In Fig. 9(b), which applies to the laser shown in Fig. 2(a), the theoretical Gaussian curve ($\exp(-r^2/a^2)$, a being the beam radius where the field amplitude falls to $1/e$, and r the distance from the beam axis) agrees quite closely with the measured values. Figs. 10(a) and (b) show amplitude distribution curves for the laser in Fig. 3(a); in these an unexplained lack of symmetry appears.

VII. DETERMINATION OF PROPERTIES OF OPTICAL ELEMENTS

In addition to measuring the signal laser's optical wavefront, it was also possible to determine the effects of putting a lens in the signal beam. Results of this experiment are described.

To facilitate measurement of lenses, the signal beam was also collimated so that now both beam wavefronts were planar. Under these conditions, placing a glass lens in the signal laser beam produced a phase-front at the collection aperture dependent on the focal length of the lens. The experimental arrangement is shown in Fig. 11 and the results of measurements on a 86.6-cm focal length lens are shown in Fig. 12. The measurements agree quite closely with the theoretical values.



$$I(r) = \frac{2P_0 e^{-2r^2/a^2}}{\pi a^2}$$

P_0 = TOTAL POWER OUTPUT

$I(r)$ = INTENSITY (WATTS/CM²) AT DISTANCE r FROM BEAM CENTER

a = BEAM RADIUS AT WHICH INTENSITY FALLS TO $1/e^2$

$2a$ = BEAM DIAMETER

Fig. 8—Intensity distribution of Gaussian curve.

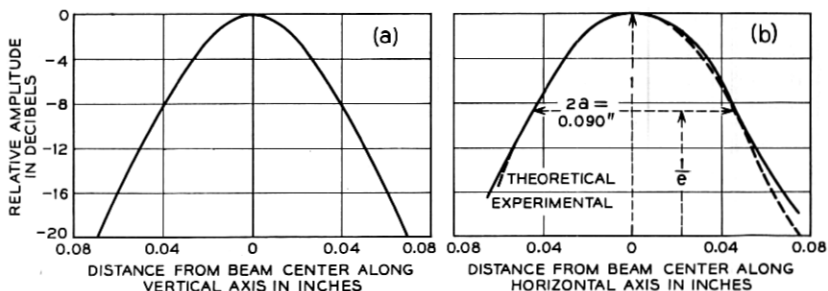


Fig. 9—Optical wavefront—amplitude (laser in Fig. 2(a), 0.009-inch collection aperture).

VIII. POSSIBLE IMPROVEMENTS

In Fig. 11 it can be seen that the lens being tested is common to both the phase-lock loop branch and the phase and amplitude measuring system. To phase-lock the loop, the two beams must be made coincident at the photomultiplier. A fixed device, such as glass lens, can be inserted in the system, the beams aligned and the loop locked. However, if the item under test introduces random variations which displace the beams relative to each other, the phase-lock loop is affected and meaningful measurements are not possible. To eliminate this problem, the setup shown in Fig. 13 is preferable. Under these conditions, the phase-locked loop is independent of the component under test and is therefore, not affected by any instability introduced. This method may require lasers with greater output powers because of the additional beam splitters required.

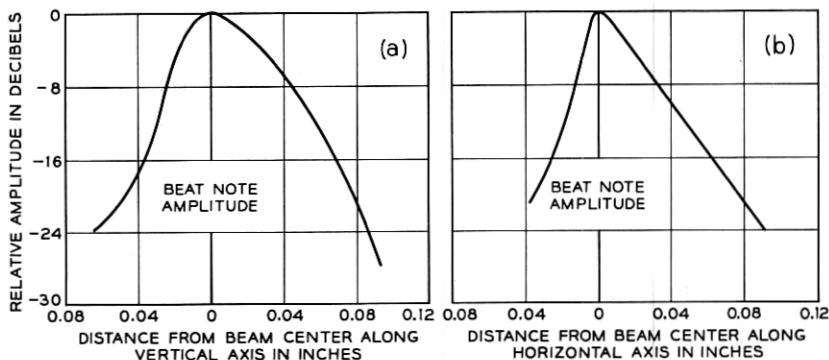


Fig. 10—Optical wavefront—amplitude (laser in Fig. 3(a), 0.009-inch collection aperture).

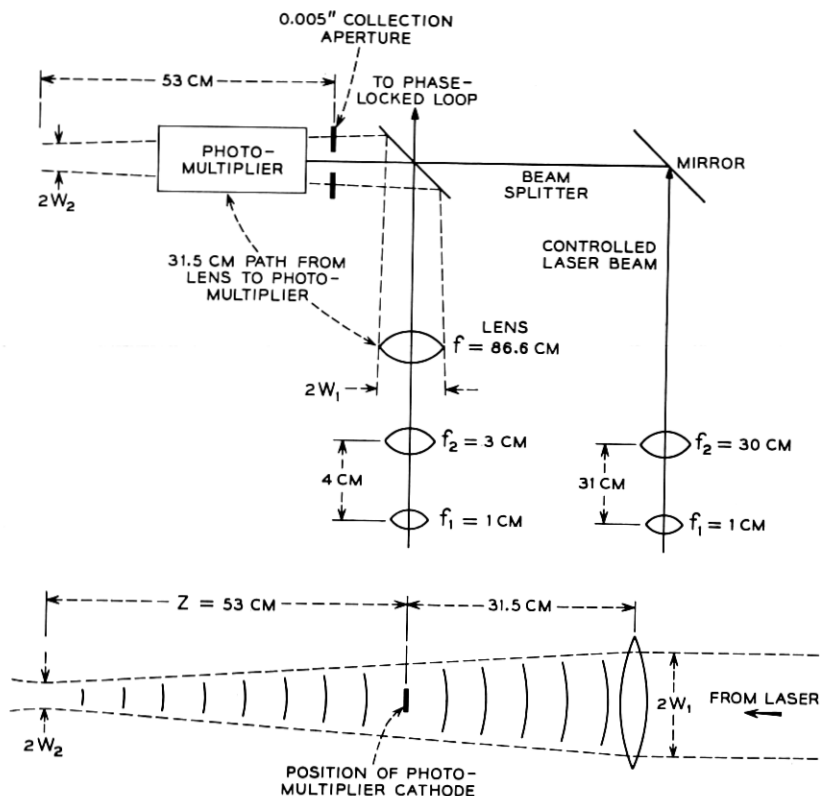


Fig. 11 — Experimental arrangement.

The system as it stands is sensitive to acoustic noises and for accurate phase measurements the laser must be maintained within a vault.¹ Enclosure in the vault permits phase-lock to be maintained for periods of 2 or 3 hours, with occasional tuning adjustments of the laser by means of the transducer-mounted mirror. Under these conditions the phase-lock is sufficiently stable to permit measurements without too much difficulty; however, it would be desirable to have portable lasers that could be used under less ideal conditions than a closed vault. Use of a transducer with a higher resonant frequency and additional gain in the feedback loop should increase the phase-lock stability.

IX. ACKNOWLEDGMENTS

Suggestions by L. H. Enloe were valuable, as were talks with J. L. Rodda, O. E. DeLange, A. F. Dietrich, T. Li, and W. H. Steier. C. P.

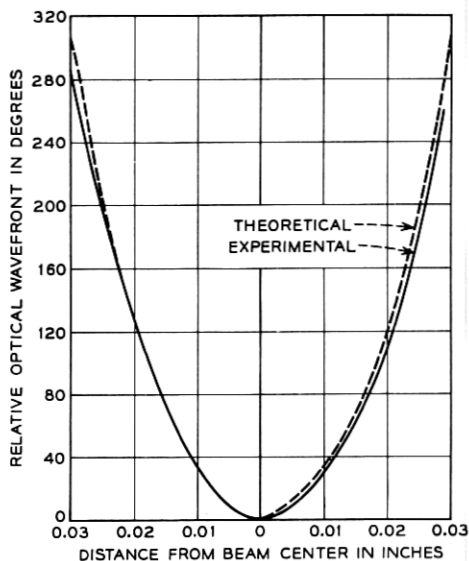


Fig. 12 — Phase front produced by a 86.6-cm focal length lens.

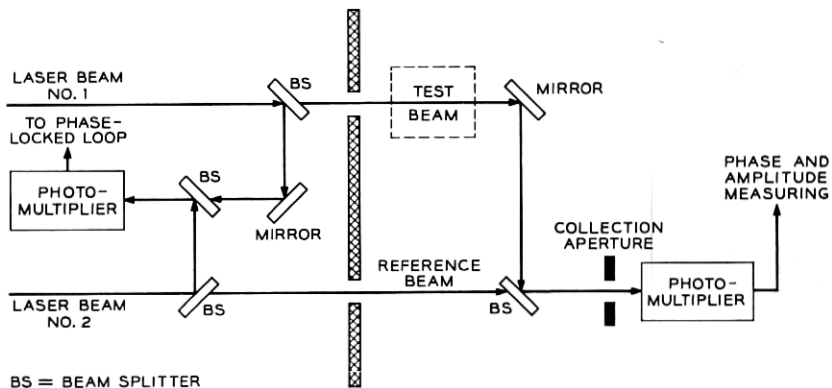


Fig. 13 — Proposed improved system.

Frazee's assistance on mechanical design was very helpful. The laser tubes were provided by E. I. Gordon of Bell Telephone Laboratories.

APPENDIX A

Calculation of Beam Waists and Spot Sizes

The following notations, some of which have already appeared, will apply in the following development:

w = spot radius, defined as the radius at which the field amplitude falls to $1/e$ of its maximum value on the z -axis.

w_0 = beam waist, which is the minimum spot radius.

w_1, w_2 = spot radii at their respective mirrors.

R_1, R_2 = radii of curvature of the two laser mirrors. One of the references⁴ uses b_1 and b_2 as the notation for the radii of curvature of the mirrors.

d = separation of two laser mirrors.

d_1, d_2 = distances to mirrors as shown in Figs. 2 and 3.

λ = wavelength = 6328\AA .

The beam waist w_0 is given by the following³:

$$w_0^2 = \frac{\lambda \sqrt{d(R_1 - d)(R_2 - d)(R_1 + R_2 - d)}}{\pi(R_1 + R_2 - 2d)}. \quad (2)$$

Output spot sizes were calculated using⁴

$$\left(\frac{w_1}{w_2}\right)^2 = \frac{R_1}{R_2} \cdot \frac{R_2 - d}{R_1 - d} \quad (3)$$

and

$$(w_1 w_2)^2 = \left(\frac{\lambda}{w}\right)^2 \frac{R_1 R_2 d}{R_1 + R_2 - d}. \quad (4)$$

Locations of the beam waists were obtained from⁴

$$d_1 = \frac{(dR_2 - d)}{R_1 + R_2 - 2d} \quad (5)$$

and

$$d_2 = \frac{(dR_1 - d)}{R_1 + R_2 - 2d}. \quad (6)$$

To compute the apparent beam waist location, it is necessary to first correct for the negative lens effect of the output mirror.⁵ The output mirror acts like a negative lens transforming the phase front of the light wave emerging from the mirror. A mirror with a radius of curvature R and an index of refraction n transforms the phase front so that the radius of curvature is R/n . In this case (Fig. 2(a)), $R = 2\text{ m}$, $n = 1.46$ (quartz) so that the new radius of curvature

$$R' = R/n = 2/1.46 = 1.37\text{ m}.$$

With this radius of curvature, using⁵

$$z = \frac{R'}{1 + \left(\frac{\lambda R'}{\pi w_2^2}\right)^2}, \quad (7)$$

the apparent beam waist appears to be at distance $z = 23.8$ cm from the output mirror; this places the apparent beam waist 6 cm outside the laser as shown in Fig. 2(a). Similar computations produce the apparent beam waist location for the other lasers as indicated in their respective figures. The radius of the apparent beam waist is obtained using the value of R_2/n rather than R_2 in (2).

APPENDIX B

Phase Relationships of Phase-Locked Loop

It has been shown when the field at the photomultiplier is $E = E_c \cos \omega_c t + E_u \cos \omega_u t$ that the difference frequency term is $E_c E_u \cos (\omega_c - \omega_u)t$ where ω_c and ω_u are the respective angular frequencies of the controlled and uncontrolled laser beams. To determine the phase relationships in the dc system, the field amplitudes are omitted and the angular frequencies and their phases are expressed as

$$\cos [(\omega_c t + \varphi_1) - (\omega_u t + \varphi_2)] = \cos [(\omega_c - \omega_u)t + \varphi_1 - \varphi_2].$$

Let

$$(\omega_c - \omega_u) = \Delta\omega \quad \text{and} \quad \varphi_1 - \varphi_2 = \Delta\varphi$$

then the error signal from the photomultiplier is

$$\cos (\Delta\omega \cdot t + \Delta\varphi).$$

When the system is phase-locked, the frequency difference $\Delta\omega \cdot t$ is equal to zero, therefore,

$$\cos (\Delta\omega \cdot t + \Delta\varphi) = \cos \Delta\varphi.$$

This, in turn, can be written as $\sin (90^\circ - \Delta\varphi)$; the error signal for the phase-lock laser loop. At phase-lock, this error voltage approaches zero and $\Delta\varphi$, the phase difference, is equal to $90^\circ \pm \alpha$, where α is the instantaneous phase error of the loop. The output of the phase detector is proportional to $\sin \alpha$ and since α is small, $\sin \alpha \doteq \alpha$, the dc error voltage is proportional to the phase difference.

When the system was modified to permit the use of a 2-MHz intermediate frequency, an additional phase detector was utilized to develop an error signal based on the output difference frequency term of the photomultiplier and a 2-MHz reference signal. Computations similar to the above show that the output error voltage of the IF phase detector is also proportional to the phase difference between the 2-MHz beat

frequency from the photomultiplier and the reference frequency of 2-MHz.

APPENDIX C

Beam Transformation Using A Telescope

The location of the output beam waist after passing through a telescope consisting of two lenses with focal lengths f_1 and f_2 , spaced at a distance $d = f_1 + f_2 \pm d$, is as follows,² where it is assumed the telescope is adjusted so that the misadjustment Δd is approximately equal to zero.

$$S_2 = - \left[(S_1 - f_1) \frac{f_2^2}{f_1^2} + f_2 \right]$$

where S_1 is the distance from the input beam waist to the first lens and S_2 is the distance to the output beam waist from the output lens. Since we know S_1 , substitution of the values for the reference telescope [$f_1 = 1$ cm and $f_2 = 30$ cm] gives us a value of 270 m for S_2 .

The radius of curvature of the wavefront is²

$$Rz = z \left[1 + \left(\frac{z_0}{z} \right)^2 \right],$$

where $z_0 = \pi w_0^2/\lambda$ and z is the distance from the output beam waist to the photomultiplier [in this case $z = S_2 - 3$ m = 267 m]. Thus, R_z is determined to be approximately 2000 m which for our purpose is considered to be a planar phase front. Since there is a good possibility that the lens arrangement is not well adjusted, it is wise to observe the output beam of the telescope over an extended distance to insure that there is no noticeable divergence or convergence of the beam diameter.

REFERENCES

1. Enloe, L. H. and Rodda, J. L., Laser Phase-Locked Loop, Proc. IEEE, Feb., 1965, 53, p. 165.
2. Kogelnik, H., Imaging of Optical Modes—Resonators with Internal Lenses, B.S.T.J., 44, March, 1965, pp. 455-494.
3. Kogelnik, H., Modes in Optical Resonators, in *Advances in Lasers*, edited by A. K. Levine, Dekker Publishers, New York (to be printed).
4. Boyd, G. D. and Kogelnik, H., Generalized Confocal Resonator Theory, B.S.T.J., 41, July, 1962, pp. 1347-1369.
5. Fork, R. L., Herriott, D. R., and Kogelnik, H., A Scanning Spherical Mirror Interferometer for Spectral Analysis of Laser Radiation, Appl. Opt., 3, December, 1964, pp. 1471-1484.

